Title
REVIEW OF WIND PRESSURE DISTRIBUTION AS INPUT DATA FOR INFILTRATION MODELS

Authors
Kula, H.G.
Feustel, H.E.

Publication Date
1988-12-01

Lawrence Berkeley Laboratory
UNIVERSITY OF CALIFORNIA

APPLIED SCIENCE DIVISION

Review of Wind Pressure Distribution as Input Data for Infiltration Models

H.-G. Kula and H.E. Feustel

December 1988

APPLIED SCIENCE DIVISION

Prepared for the U.S. Department of Energy under Contract Number DE-AC03-76SF00098.

DISCLAIMER

LBL-23886

Review of Wind Pressure Distribution as Input Data for Infiltration Models

Hans-Georg Kula and Helmut E. Feustel

Indoor Environment Program
Applied Science Division
Lawrence Berkeley Laboratory
Berkeley, CA 94720, U.S.A.

December 1988

This work was supported by the Assistant Secretary for Conservation and Renewable Energy, Office of Building and Community Systems, Building Systems Division of the U.S. Department of Energy under Contract No. DE-AC03-76SF00098, and Carl-Duisberg-Gesellschaft e.V. (Cologne, Federal Republic of Germany) Program No. P-3-5012.

Abstract

Previous investigations have shown that the pressure difference between the inside and outside of the building is one of the driving forces for air infiltration. This pressure difference mainly depends on the wind and its interaction with the envelope of the building which is commonly expressed as dimensionless pressure coefficients. The main part of this report is a literature review on the wind pressure distribution around the building, with emphasis on high-rise buildings. Reports of single family buildings were also reviewed and evaluated. In the second part of this paper, an examination of wind pressure distribution curves on the centerline of the windward and leewardside of the building was done and a polynomial fit is presented. This set of coefficients covers a wide range of buildings of varying heights and varying plan area densities.

1. Introduction

The primary means of indoor air quality control is the exchange between the air inside a building with the outside air and energy use associated with the conditioning of the outside air. The air exchange can either be intentional (ventilation) or unintentional (infiltration). Indoor air quality in U.S. residences is mainly maintained by infiltration.

Air infiltration is the uncontrolled flow of air through openings in the building surface. As infiltration is the consequence of pressure differences between the inside and outside of the building due to wind and thermal buoyancy (stack effect), the air exchange for a given building can easily vary by an order of magnitude. In order to reduce excess infiltration rates, buildings are being built tighter to prevent unnecessary heating and cooling losses. As the infiltration is linear dependent on the tightness of a building, cutting excess infiltration rates also reduces infiltration at low pressure situations.

The ventilation rate necessary to provide acceptable indoor air quality in residential buildings has been determined to be in the range of 0.35 ach to 1.0 ach [2,3] In tight buildings, however, it might not be possible to maintain acceptable indoor air quality by means of infiltration only. Therefore, mechanical ventilation systems might become necessary.

In order to determine ventilation rates for multizone buildings for given weather conditions, Lawrence Berkeley Laboratory has developed a simplified infiltration model. The amount of infiltration experienced by a building depends on the leakage areas of the building, the leakage distribution, the temperature differences between inside and outside the building, the wind speed and wind direction, as well as the roughness and density of the building's surrounding. Whereas reasonable results for leakage area and temperature differences can be obtained by in-situ measurements, the wind pressure distribution around a building cannot easily be measured due to rapid changes of wind speed and wind direction. Because of these rapid wind changes, accurate data for the wind pressure fields can only be obtained by performing wind tunnel measurements on scale models of the considered building and its surroundings.

To calculate the infiltration rate of a building it is necessary to predict the wind pressure distribution. Investigations dealing with the wind pressure distribution on buildings were usually performed to predict static and dynamic wind loads on the structure of the building, rather than for infiltration purposes. For structual load calculations only the maximum forces are important, whereas for air infiltration calculations the mean value for given weather conditions are important.

The knowledge of the pressure distribution for simulation purposes is of special interest for multistory buildings, especially if their height significantly exceeds the surrounding buildings. Figure 1 shows the comparison of calculated pressure differences for several vertical pressure profiles found in the literature [4]. These profiles are calculated for a nine-story dormitory located next to the University of California campus in Berkeley. Whereas the surface pressure profile proposed by ASHRAE [1] is constant over the building height, all other profiles investigated show a dependence on the height above ground. The influence the pressure profile has on the pressure differences causing an air flow between outside and the staircase is shown in Figure 2 for two selected stories. Whereas all pressure profiles for the eighth floor show a similar tendency of the pressure differences on the windspeed, pressure differences vary significantly with the windspeed for the ground floor, depending on the chosen profile. This is particularly evident for the profile suggested by ASHRAE in comparison with those from Hussain and Lee, and Krischer and Beck. This example may show, how important the accurate description of the pressure field around buildings is for simulating a building's infiltration rate. The task of this report is to summarize research results on pressure distributions around buildings found in the literature with an emphasis on multistory buildings. An attempt is made to find simple algorithms to describe the pressure distribution around buildings in different surroundings.

2. Physical Fundamentals of Wind Pressure Distribution

Wind pressure is one of two main driving forces for natural ventilation. Differences in the temperature of the earth surface due to solar radiation cause global pressure differences in the atmosphere. Compensation for these pressure differences causes the flow of enormous amounts of air from regions of high pressure to regions of low pressure. The direction of this air flow (i.e., wind) depends on the pressure gradient, coriolis force, and friction on the earth's surface.

The shear layer formed by the action of shear stress at a solid boundary is called boundary layer. The velocity in that shear layer goes from zero at the surface of the solid boundary up to the velocity of the free stream at the outer edge. The flow in the region between both limits is dominated by the effect of viscosity. Depending upon the Reynolds number, the flow in this region is either laminar or turbulent. Wind flow is characterized by turbulent boundary layer flow with a thickness of a few hundred meters.

When a boundary layer flow hits a sharp edge, such as a corner of a rectangular building, the separation occurs immediately. A description of the influence of the Reynolds number on the separation at sharp edges and round corners is given in Figure 3. As it can be seen in Figure 3a, the effect of the Reynolds number is

neglectably small for rectangular buildings, because it is no longer the dominating factor in controlling the separation and wake width [5].

There are a number of variables affecting the pressure distribution around a building due to natural wind. The main source of information about the interaction between these parameters comes from work performed on scale model experiments in wind tunnels. Buildings in urban areas are often built so close together that they can be considered as a single entity. This makes a single building less important than the design of the flow channels formed by all the buildings in the group.

The vertical profile of the wind speed in the atmospheric boundary layer is primarily dependent upon the roughness of the surface surrounding the building. The wind speed increases with the increasing height above ground. The wind velocity profile can be calculated either by a logarithmic equation

$$\frac{v(z)}{v(z_0)} = \frac{\ln z - \ln z_r}{\ln z_0 - \ln z_r} \tag{1}$$

or a power law expression

$$\frac{v(z)}{v(z_0)} = \left\{\frac{z}{z_0}\right\}^{\alpha} \tag{2}$$

with:

v	wind velocity at height z $[m/s]$
z	height above ground $[m]$
z_0	reference height for wind velocity measurements $[m]$
z_r	roughness height, depends on roughness of environment $[m]$
α	exponent [-]; value depends on terrain roughness

Equation 2 is most often used by engineers and building scientists. Both equations assume that the wind flow is isothermal and horizontal. An assumption is made that the wind flow will not change its direction as a result of differences in the terrain surface. The value of the exponent α increases with increasing roughness of the solid boundary. Figure 4 shows the wind profile for three selected types of surrounding roughness. For smaller areas of rough surfaces in a more smooth surrounding, such as a town located in flat, open surroundings, the velocity profile described by Eq's. 1 and 2 is only valid for a limited height above the obstacles. The wind velocity well above the small town is determined by the roughness of its surroundings.

Table 1: Height of boundary layer and exponents for different surrounding roughness [6]

roughness type	height of boundary layer [m]	exponent α [-]
flat open country	270	1/7.0
rolling hills	390	1/3.5
inner city areas	510	1/2.5

Wind flows produce a velocity and pressure field around buildings. The relationship between velocity and related pressure at different locations of the flow field can be obtained from the dynamics of a particle in the fluid. For freestream flow, Bernoulli's equation provides the answer for the relationship between pressure and the velocity field. Bernoulli assumes steady state flow in a regime where viscous forces are negligible. The resultant equation is the most important expression for gaining an understanding of fluid behavior [5].

$$p_1 + \frac{1}{2}\,\rho\,\bar{v}_1^2 + \rho g z_1 = p_2 + \frac{1}{2}\,\rho\,\bar{v}_2^2 + \rho g z_2 \tag{3}$$

with:

g	acceleration of gravity $[m/s^2]$
p	pressure $[Pa]$
ρ	density $[kg/m^3]$

For subsonic aerodynamic problems, the gravitational term of the equation is negligible in most cases. Assuming constant density at a given temperature, Bernoulli's equation can be simplified to:

$$p + \frac{1}{2}\rho\bar{v}^2 = const \tag{4}$$

This means that a decrease in velocity is accompanied by an increase in pressure, and vice versa.

When compared to the static pressure associated with an undisturbed wind-velocity pattern, the pressure field around a building is generally characterized by regions of overpressure on the windward side (drop of velocity), and underpressure on the facades parallel to the air stream on the leeward side of the building. As Bernoulli's equation is only valid for the aforementioned assumptions,

boundary layer flows and shear flows (where viscous effects are significant), like those on the facades parallel to the air stream, are not covered by this equation.

The pressure distribution around a building is usually described by dimensionless pressure coefficients -- the ratio of the surface pressure and the dynamic pressure in the undisturbed flow pattern. The pressure coefficient at point k can be described by:

$$c_k(x,y,z,z_{ref},\phi) = \frac{p_k(x,y,z) - p_0(z)}{p_{dyn}(z_{ref})} \tag{5}$$

with

$$p_{dyn}(z_{ref}) = \frac{1}{2}\,\rho_{out}\,v^2(z_{ref}) \tag{6}$$

where:

c_k	pressure coefficient for surface element k [-]
p_k	pressure at surface element k $[Pa]$
p_0	atmospheric pressure $[Pa]$
p_{dyn}	dynamic pressure in the undisturbed flow $[Pa]$
x,y,z	coordinates $[m]$
ρ_{out}	density of the outside air $[kg/m^3]$
z_{ref}	reference height for wind velocity $[m]$
ϕ	wind direction [-], usually 10 m above ground

The reference height is often chosen to be 10 m above ground; however, pressure coefficients can be based on the wind speed at the considered height, at the height used for the wind speed measurement, at the building height or at the height of the boundary layer. Since many basis are chosen, comparison of data found in literature is bothersome. Pressure coefficients at one of the above bases can be converted into other coefficients with another basis, using the expression:

$$\frac{c_1}{c_2} = \left(\frac{z_2}{z_1}\right)^{2\alpha} \tag{7}$$

with

c_1	pressure coefficient at height 1 [-]
c_2	pressure coefficient at height 2 [-]
z_1	reference height 1 $[m]$
z_2	reference height 2 $[m]$

3. Literature Review

3.1 Type of Measurements

3.1.1 Full Scale Measurements

In recent years, a number of full scale measurements of wind effects on tall buildings have been carried out [7-11]. Full scale studies provide investigations with new approaches and ideas, show the sensitivity of the different types of wind and give the necessary results to validate measurements obtained in wind tunnels. It is hoped that the results obtained will help to develop generalities from full scale observations as well as present material for the verification of theories and models.

The particular structure of the building and its unique surroundings presents several difficulties in carrying out full scale investigations. Another problem is the instrumentation of the building. As the wind changes not only its velocity but also its direction, all the measurements for one cycle have to be taken at exactly the same time, which is impossible with a reasonable amount of measurement equipment. Another problem concerning the measurements is to find a point to measure the reference static pressure. One of the several recommendations mentioned in literature to measure the reference pressure during full scale measurements is a pitot-static probe installed on a mast. Furthermore, spread over the whole building, it is difficult and also expensive to have enough points to measure, and in most of the cases, the instrumentation has to be built specially for the building being looked at. All full scale measurements are time consuming. The relatively infrequent opportunity for observation of strong winds generally makes the experiment either of long duration or incomplete.

3.1.2 Wind Tunnel Measurements

A common method to investigate wind pressure distribution is to carry out wind tunnel measurements on scale models of buildings and their surroundings. To model the turbulent flow induced by buildings, it is necessary to place the scale model of the building in an air stream, which as a minimum must reproduce the correct mean velocity and turbulence intensity profiles [5].

There are several advantages for wind tunnel investigations. The conditions for these tests are consistent and reproducible. Different wind directions can be simulated by locating the building model on a turn table. The influence of various obstacles in the building's surrounding can be determined by changing the model set up. Unfortunately, it is not yet possible to fulfill all conditions to simulate the air flow in the atmospheric boundary layer, but results are considered to be accurate for further calculations. Table 2 shows the conditions of wind and its possibility of fulfillment in a boundary layer wind tunnel.

3.2 Overview of Research Work

3.2.1 Single-Family Buildings

Several wind tunnel investigations have been carried out to analyze the pressure distribution around single-family buildings. Almost all of these investigations give a complete picture of the wind pressure distribution including the influence of other buildings in the vicinity and wind breaking obstacles like hedges and wooden fences.

Based on wind tunnel measurements of Flachsbart [12], Krischer and Beck [13] suggest simplified wind pressure distributions for perpendicular wind flow and wind flow 45 ° to the perpendicular to simulate infiltration in single family buildings. For flow perpendicular to a building's facade they suggest pressure coefficients of $c = 1.0$ for the windward side and $c = -0.3$ for the other three facades. These pressure coefficients are based on the undisturbed wind speed at the height of interest.

The most complete report on the wind pressure distribution for single-family buildings has been published by Wiren [14], who describes a wind tunnel study of a 1:100 scale model of a 1½-story single family house in different surroundings. The exponent α for the profile of the approaching wind has been chosen to be 0.14, which simulates open surroundings. The influence of adjacent buildings was simulated by using different layout patterns. Pressure coefficients were referenced with respect to roof height. Figures 5 and 6 describe the pressure distribution found by Wiren for the two wind angles of 0 ° and 45 °. The plots also show results from Krischer and Beck converted to the height of the Wiren measurements [13].

Wiren shows that adjacent houses have a large effect on the magnitude and distribution of wind pressures over a single-family house. Two or more houses placed upwind have little additional effect on the pressure over the windward surfaces at the angles $\beta < 60$ °. The effect on the leeward side is to decrease the under-pressures at angles between 0 ° and 60 ° and to increase the pressures if the angle of the approaching wind is larger then 60 °. The effect of two houses placed side by side upwind are most pronounced on the facade walls and on the leeward gable wall in both cases at wind angels between 0 ° and 60 ° [14]. All results obtained by Wiren show higher pressure coefficients then the results proposed by Krischer and Beck.

In their study Wilson and Kiel [15] made calculations for the wind shielding factor C', to determine the effects of building shape and wind direction. Wilson distinguishes two different typs of shelter. The difference between the two types of shelter can be described by the distance between the buildings. If the obstacles are numerous and more than five times their height away from the building, their indirect effect on wind shelter is to lower the wind speed U_c approaching the

building. U_c is the windspeed at ceiling height measured in an unobstructed location in the same terrain in which the building is located. This type of shelter is dealt with when classifying the terrain as urban, suburban or rural. The second type of shelter is from obstacles which are closer to the building than five times their height. The wake downwind lowers the stagnation pressure on the upwind wall. This direct local shelter may be accounted for by adjusting the shielding coefficient C' or by a further correction to the effective approach speed U_c.

The report by Vickery et. al. [16] presents the results of a set of wind tunnel tests for low rise buildings in open as well as in suburban terrains. For three different wind angles (0, 45, and 90 °) tests were carried out with a scale model that had a plan dimension of 24 x 38 m. The height was varied three times: (5 m, 7 m and 10 m) the roof slopes were 1:12, 4:12 and 12:12.

Full scale investigations made by K. Handa [17] present results of pressure measurements on a typical Swedish timber house. The test house is located in an area with a few buildings on one side and low hills on the other, which represents open and semi urban site conditions. The rate of air infiltration has been calculated by employing the values obtained from full scale pressure distribution, air leakage characteristics and temperature differences. The results are compared with the actual ventilation obtained from tracer gas measurements.

3.2.2 Multistory Buildings

As mentioned earlier, most of the investigations dealing with wind pressure distribution on the surface of high rise buildings are performed to predict the load on the structure due to wind (gust, thunderstorm) [18,19,20]. Few data are available to predict the pressure distribution for calculations of air infiltration or natural ventilation [21].

A good collection of pressure coefficient data has been obtained by Hussain and Lee in investigations carried out 1980 [22,23,24]. In three different investigations they measured surface pressure coefficients on models of different size, and different surroundings in an atmospheric boundary layer wind tunnel. They measured the vertical pressure distribution on the centerline of the model. In these reports pressure coefficients are generally normalized with respect to the velocity of the gradient wind, which in their cases occurred at a height of 22 times the cube height. The height of one cube was 0.036 m. They provided a wind velocity profile with a flow exponent $\alpha = 0.28$ to simulate the atmospheric wind flow in an urban area. In their first report [22] they describe test results using an isolated cube, varying the height ratio from 1 to 4, the frontal aspect ratio from 1 to 4 and the side aspect ratio from 1 to 2. The height ratio is measured relative to the height of the cube/roughness element height. The frontal aspect ratio is the ratio

of the length to the height of the building, the side aspect ratio is the ratio of the width to the height. The results obtained with the testing of the isolated cube are regarded as 0 % plan area density, which means no adjacent buildings have been taken into account. In Figure 7, the variation of the mean windward and leeward pressure coefficient is shown plotted against the frontal aspect ratio A_f. Figure 7 shows that both the windward and the leeward pressure coefficient vary as the frontal aspect varies. The variation of the side aspect ratio A_s presents a different picture of the flow around various models. Figure 8 shows that the mean windward pressure coefficient remains the same within the range of values of A_s considered in this investigation. The mean leward pressure coefficient, on the other hand, changes as the side aspect ratio varies from 0.5 to 1.5, after which it tends to become constant [12].

During their second investigation [23] measurements of the flow over large arrays of identical roughness elements and the effect of frontal and side aspect ratio variations were measured. The result is the introduction of three different flow regimes, dependent on the value of the element spacing and the plan area density. During this second investigation they varied the plan area density (PAD) between 3.125% and 50% (for definition see Figure 10).

The aim of the third investigation was to determine the effect of central model height variations relative to the surrounding roughness arrays [24]. Therefore, the height was varied from 0.5 to 4.0 relative to the height of the surrounding roughness elements. The plan area density was also varied during that investigation. For the normal pattern values from 5.0% to 25% were chosen, whereas for the staggered pattern the values chosen ranged from 10% to 40%. The pressure distribution on the windward side was found to be similar to the pressure distribution for the cube in various densities. For the isolated roughness flow regime the pressure profile could be described as "S" shaped, changing to an "reversed C" shape in the wake interference and the skimming flow regimes. The "reversed C" shape of the profile changed back to an "S" shape for models of heights larger than the thickness of the inner boundary layer of the array [24]. The inner boundary layer profile outgrows the element arrays and results in different inner layer velocity profiles in each density which have different effects on the overall pressure. The leeward pressure distribution profiles were found to be non-uniform. These profiles for models having a relative height > 2.0 showed a distinct kink at the average height of the array.

In his investigation, Bowen [25] describes the wind pressure distribution by using simple building models of a scale of 1/400, which represent buildings with a plan area of 31 x 46 m and a varying height of 15 m, 31 m, 61 m and 92 m. This corresponds with a plan area density (PAD) of 30% and relative building heights of 1.0, 2.0, 4.0 and 6.0. By using a power law equation with an exponent of 0.43 for the simulation of the wind profile he simulated a high urban density area.

Wind angles from 0 ° to 135 ° were modeled. There were seven pressure measurement taps on the longer sides of each models and five on the shorter sides. The pressure coefficients were related to the dynamic pressure of the flow at the top of each building. The maximum local vertical pressure coefficient in the centerline reached 0.96 at an relative height of the model of 0.85 and a wind angle of 0 °. These high coefficients were rapidly reduced towards the eaves and the corner of the model. Coefficients at the leeward side of the building were fairly uniform between -0.35 and -0.45.

It is very difficult to compare results from different investigations because of the many different parameters chosen by each investigator for their particular purposes. Different parameters in these two reports are the power law exponent of the approaching flow. Bowen chose 0.43 for *high density urban area* whereas Hussain and Lee chose 0.28 for *urban terrain.* Hussain and Lee varied the plan area density during their investigation from 5% to 25% for the normal pattern and from 10% to 40% for the staggered pattern. Bowen, however, tested only the normal pattern with a plan area density of 30%. Another different aspect is the plan area of the models. Hussain and Lee tested with square models whereas Bowen tested with rectangular models. Nevertheless, the results obtained in the two investigations look similar for the cases that were compared. Both profiles for the vertical pressure distribution in a high plan area density, Hussain and Lee 25% and Bowen 30% show the same "S" shape. The highest pressure coefficient values occur in both investigations at a relative height of 0.825 and 0.85 with a c value of 0.96. At the bottom of the models the pressure coefficient are not similar, probably due to the different plan area density and, therefore, different flow quality.

The report by Akins and Cermak [28] presents a comprehensive set of wind tunnel tests with flat-roofed rectangular building models. Four different boundary layers were used, simulated by exponents of 0.12, 0.26, 0.34 and 0.38. The pressure coefficients obtained were referenced with respect to the local velocity at the point of measurement. This procedure made the pressure coefficient independent of height and boundary layer profile. The results of the wind tunnel tests are listed in tables or plotted in graphs. One of the conclusions is that the mean local pressure coefficients for corresponding locations and wind directions for isolated flat-roofed rectangular buildings are primarily dependent on the side ratio of the building. Results for different aspect ratios and different approach flow conditions may be satisfactorily condensed to one set of mean local pressure coefficients for each side ratio and wind direction [28].

The report by Swami and Chandra [29] describes procedures for calculating natural ventilation airflow rates in buildings, because natural ventilation through open windows could be an effective cooling strategy. In the first part of their report they describe procedures for a single window, for one inlet and one outlet

and for ventilation through multiple inlets and outlets. They compare measured ventilation rates with their prediction and obtained accurate results. As one of the driving forces for ventilation is the pressure distribution around a building, the second part of their report is an analysis of the worldwide database on building pressure distribution for low- and high-rise buildings. Based on a curve fit of experimental data collected from different sources they obtained two sets of equations to calculate pressure coefficients. For different surroundings and other effects they give correction and modification values for the pressure coefficient [29].

4. Findings

4.1 General

The aim of this report was to determine input data for air infiltration models. As we learned from the literature review, the pressure distribution of a building depends on several parameters. The pressure distribution for each of the facades of a building forms a three dimensional curve. Its shape is a function of the wind profile, the building height, the building's environment, and the wind direction. In order to describe the measured pressure distribution for each of the facades of the building's envelope, a multi-dimensional array with all the data points obtained in wind tunnels tests has to be stored in a file. Since this is not a very practical solution, we decided to try to describe the three dimensional pressure field by the vertical distribution of the surface pressure for the center of the facade at wind direction perpendicular to the windward side and a set of curves describing the horizontal pressure distribution for several heights above ground and different wind directions.

Unfortunately, all of the articles reviewed describe significantly different test setups. Therefore, only a few of the investigations necessary to describe the pressure field around buildings comprehensively have been performed. Therefore, we had to decide to either describe the pressure distribution for a single surrounding but different wind directions, or for different surroundings and only the vertical pressure distribution at winds perpendicular to one facade of the building, or for different wind directions and aspect ratios but no surroundings at all.

In order to get the full picture on the pressure distribution around buildings for all the different influences, one needs either more data or an algorithmns which describes the different dependencies. Not being able to perform wind tunnel measurements, which would fill the gaps of knowledge, we decided to investigate further in the mathematical function of the vertical pressure distribution at perpendicular winds. This decision was made on the fact, that Hussain and Lee [22,23,24] published the most comprehensive study for our purpose.

4.2 Vertical Distribution of Surface Pressure, Windward Side

The results shown in the following section were considered for perpendicular flow in the location of the vertical axis of the building. To determine the vertical pressure distribution the data obtained by Hussain and Lee [22,23,24] was used. An attempt was made to find a relatively simple way to describe the pressure distribution on the windward and leeward side of the building by means of using only few data necessary to store. As described before, all of the vertical pressure distributions considered can be described as "S-shaped" or as "reversed C-shaped". The first attempt to describe the pressure distribution curves obtained by Hussain and Lee was made by using up to four straight lines. As this method did not show sufficient accuracy no further effort was made in this direction. Further investigation showed, that both curve types could be described by polynomial functions of higher order. Tests for selected vertical distribution profiles showed sufficient agreement when described by 3rd order polynomial functions. The values obtained by Hussain and Lee were used as input data to determine the coefficients for the 3rd order polynomial with the help of a curve fitting program. Figures 11-14 are plots of this curve fit. Each plot shows the pressure distribution for one plan area density (PAD) in the normal pattern (0%, 5%, 12.5% and 25%) for a sample of different relative heights of h = 1, 2 and 4. Figure 10 shows, how the different plan area densities had been calculated [22]. In these plots the dependence of the pressure coefficient on the relative height of the building can be seen. The curves of the pressure distributions at the same relative heights in Figures 11-14 (e.g. h = 4) are quite similar at the upper level of the building. At the bottom of the building it changes due to the density of the plan area. The pressure coefficients at the bottom get smaller with an increase of the plan area density.

The above-mentioned aspect can be found throughout all the curves. The higher the plan area density the steeper the curves. A third aspect is the fact, that there is a change in the shape of the curves from "S" shape to "reversed C" shape at a relative height between 1.5 and 1.7. The description of the pressure distribution curves at the centerline of the building with a 3rd order polynomial reduces the input data to four coefficients per curve. Results of this investigation regard the relative height of a building and the plan area density it is situated in.

$$c_p(z) = \left\{ a_0 + a_1\, z + a_2\, z^2 + a_3\, z^3 \right\} \tag{8}$$

The influence of the wind direction was disregarded. The results of this investigation are listed in Tables 3 to 20.

4.3 Vertical Distribution of Surface Pressure, Leeward Side

The same investigation made for the windward side was made for the leeward side. Because these leeward side curves were not as pronounced as the windward curves a 2nd order polynomial should give a good agreement with the raw data from Hussain and Lee. However, for three different heights of h = 0.5, 1.0 and 4.0 the coefficients were found not to be in good agreement with 2nd polynomial fit especially for a height of 4.0. Even those curves that could be matched with 2nd order polynomial were described by 3rd order polynomials to get the same kind of input data for the leeward side as for the windward side.

The leeward pressure distribution profiles found by Hussain and Lee [22-24] were found to be non-uniform. For relative heights from 0.5 to 1.2 the curves show a "reversed C" shape, changing to a flat "S" shape for heights >1.2. Over a height of 2.0 the curves show a distinct kink at the average height of the surrounding array. This is experienced throughout all plan area densities in the normal pattern. In this pattern the pressure coefficients are all negative. The highest negative value of c = -0.21 was measured at a relative building height of 0.85 at the isolated cube with a relative height of h = 4.0. The pressure coefficient values decrease as the plan area density increases. At the bottom of the model h = 0.5 situated in the stagered pattern the pressure coefficient became slightly positive. For plan area densities of 10%, 12.5% and 25% the highest positive value is c = 0.005 at the bottom of the model getting back to negative values at a plan area density of 40%. The results of this investigation are listed in Tables 3 to 20.

5. Summary

The main part of this report is a literature review about the wind pressure distribution around buildings, with emphasis on high rise buildings.

The second part is an investigation to find a method to describe the wind pressure distribution around buildings in a simple way. Pressure data are used as input for air infiltration estimations based on computer simulation models. To get a good estimate for air infiltration due to the wind pressure field around the building's envelope it is necessary to use accurate pressure values. Pressure data published by other researchers were evaluated. A curve fitting program was used to describe the wind pressure distribution curves by 3rd order polynomials. The data considered in this investigation are limited to those wind directions where flows are approaching perpendicular to the building array. Pressure coefficients were measured on the center line of the building. Further investigations are necessary to take other wind directions into consideration. To get sufficient data more wind tunnel investigation for the wind pressure distribution are necessary.

6. Literature

[1] Anon.
"ASHRAE Handbook 1985 Fundamentals"
American Society of Heating, Refrigerating and Air Conditioning Engineers, Inc., Atlanta, 1985

[2] Anon.
"ASHRAE Standard 62-1981 R: Ventilation for Acceptable Indoor Air Quality",
American Society of Heating, Refrigerating and Air Conditioning Engineers, Inc., Atlanta, 1987

[3] Le Marie, A. and Trepte, L.
"Guidelines for Minimum Ventilation Rates"
ASHRAE/DOE/BTECC, "Thermal Performance of the Exterior Envelopes of Buildings III", Clearwater, Florida, 1985

[4] Feustel, H.E. et. al.
"Temperature- and Wind- Induced Air Flow Patterns in a Staircase. Computer Modelling and Experimental Verification"
Lawrence Berkeley Laboratory, LBL-14589, August 1985

[5] Aynsley, R.M.; Melbourne, W.; Vickery, B.J.
Architectural Aerodynamics
"5.3.1 Wind Tunnel Testing Techniques", pp 163
Applied Science Publishers Ltd. 1977

[6] Davenport, A.G.
"A Rationale for the Determination of the Basic Design Wind Velocities"
ASCE-Proceedings 86 (1960), pp. 36-38

[7] Jones, P.M.; Wilson, C.B.
"Wind Flow in an Urban Area: A Comparison of Full Scale and Model Flows"
Build. Sci., Vol. 3, pp. 31-40. Pergamon Press 1968

[8] Dalgliesh, W.A.
"Comparison of Model and Full Scale Tests of the Commerce Court Building in Toronto"
Division of Building Research, National Research Council of Canada

[9] Dalgliesh, W.A.
"Comparison of Model/Full Scale Wind Pressure on a High-Rise Building"
Journal of Industrial Aerodynamics, 1 (1975), PP 55-66

[10] Gusten, J.
"Full-Scale Wind Pressure Measurements on Low-Rise Buildings
1984 Wind Pressure Workshop Proceedings"
Air Infiltration and Ventilation Centre, Technical Note AIC 13.1,
Barcknell, U.K., 1984

[11] Matsui, G.; Suda, K.; Higuchi, K.
"Full-Scale Measurement of Wind Pressure Acting on a High-Rise
Building of Rectangular Plan"
Journal of Industrial Aerodynamics, 10 (1982) 267-286

[12] Flachsbart, O.
"Winddruck auf Offene und Geschlossene Gebaeude"
Erg. der Aerody. Versuchsanstalt Goettingen
IV. Lieferung, S.515

[13] Krischer, O. and Beck, H.
"Die Durchlueftung von Raeumen durch Windangriff und der Waerme-
bedarf fuer die Lueftung"
VDI Berichte, Bd. 18, 1957

[14] Wiren, B.G.
"Effects of Surrounding Buildings on Wind Pressure Distribution and
Ventilation Losses for Single-Family Houses"
Part 1: 1½-Storey Detached Houses
National Swedish Institute for Building Research, Bulletin M 85:19

[15] Wilson, D.J.; Kiel, D.E.
"Effect of Building Shape, Wind Shelter and Openings
on Air Infiltration"
Departmental Report No. 53, University of Alberta, Canada,
October 1985

[16] Vickery, B.J.; Baddour, R.E.; Karakatsanis, C.A.
"A Study of the External Wind Pressure Distributions and Induced
Internal Ventilation Flow in Low-Rise Industrial and Domestic
Structures"
Florida Solar Energy Center, Cape Caneveral, Florida, January 1983

[17] Handa, K. and Gusten, J.
"Estimation of Rate of Air Infiltration Based on Full-Scale Wind
Pressure Measurements"
3rd AIC Conference, September 20-23 1982, London, UK

[18] Davenport, A.G. and Dalgliesh, W.A.
"A Preliminary Appraisal of Wind Loading Concepts of the 1970
National Building Code of Canada"
Technical Paper No. 405, Division of Building Research, Ottawa

[19] Kareem, A.
"Measurements of Total Loads Using Surface Pressures"
Department of Civil Engineering
University of Houston

[20] Davenport, A.G. and Isyumov, N.
"The Application of the Boundary Layer Wind Tunnel to the Prediction of Wind Loading"
Proceedings of Conference "Wind effects on Buildings and Structures", Ottawa, 11-15 September 1967, Vol. 1, pp. 201-230

[21] Kelnhofer, W.J.
"Air Infiltration in Buildings Due to Wind Pressures Including Neighboring Body Effects"
from "Heat Transfer in Energy Conservation" ed Goldstein, R.J. et al pp. 47-56, January 1977

[22] Hussain, M. and Lee, B.E.
"An Investigation of Wind Forces on Three Dimensional Roughness Elements in a Simulated Atmospheric Boundary Layer"
Part 1:
"BS 55: Flow Over Isolated Roughness Elements and the Influence of Upstream Fetch"
University of Sheffield, July 1980

[23] Hussain, M. and Lee, B.E.
"An Investigation of Wind Forces on Three Dimensional Roughness Elements in a Simulated Atmospheric Boundary Layer"
Part 2:
"BS 56: Flow Over Large Arrays of Identical Roughness Elements and the Effect of Frontal and Side Aspect Ratio Variations"
University of Sheffield, July 1980

[24] Hussain, M. and Lee, B.E.
"An Investigation of Wind Forces on Three Dimensional Roughness Elements in a Simulated Atmospheric Boundary Layer"
Part 3:
"BS 57: The Effect of Central Model Height Variations Relative to the Surrounding Roughness Arrays"
University of Sheffield, July 1980

[25] Bowen, A.J.
"A Wind Tunnel Investigation Using Simple Building Models to Obtain Mean Surface Wind Pressure Coefficients for Air Infiltration Estimates"
LTR-LA-209, National Research Council Canada, Dec. 1976

[26] Allen, C.
"Wind Pressure Data Requirements for Air Infiltration Calculations"
Air Infiltration and Ventilation Centre, Technical Note AIC 13,
Barcknell, U.K., 1984

[27] Davenport, A.G.
"The Relationship of Wind Structure to Wind Loading"
Proceedings of Conference "Wind Effects on Buildings and Structures"
National Physical Laboratory, 26-28 June 1963

[28] Akins, R.E. and Cermak, J.E.
"Wind Pressures on Buildings" NSF Grant ENG72-04206-A01 and ENG76-03035
Fluid Mechanics and Diffusion Laboratory, College of Engineering,
Colorado State University, CER76-77REA-JEC15 1976.

[29] Swami, M.V. and Chandra, S.
"Procedures for Calculating Natural Ventilation Airflow
Rates in Buildings", ASHRAE Research Project 448-RP
Final report FSEC-CR-163-86, March, 1987
Florida Solar Energy Center, Cape Canaveral, Florida 32920

Table 2:Similarity requirements for wind tunnel investigation [26]	
Condition	Possibility of fulfillment
1. Undistorted scaling of geometry	Yes: within limits of scale
2. Equal Rossby No.	No
3. Equality of gross Richardson No.	Yes, in metrorological wind tunnel
4. Equal Reynolds No.	No, but not to serious since most features depend weakly
5. Equal Prandtl No.	Yes
6. Equal Eckert No.	No, incompatible with matching Richardson No.. Effect is small
7. Surface roughness distribution which exhibits areodynamically rough behaviour must match	Yes, within limits that the minimum roughness exceeds $10.\nu / U^*$ (U^*= friction velocity, ν= kinematic viscosity).
8. Topographic relief	Yes
9. Surface temperature distribution	Yes, by using heating and cooling elements in the WT upstream
These approach flow conditions must be matched	
10. The distribution of mean velocities	Yes
11. The distribution of turbulent velocities, including the energy spectra	Yes for bottom 10-15 % of WT
12. The mean temperature distribution	Yes
13. Fluctuating component of the temperature distribution	Yes, in metrological wind tunnel
14. The longitudinal pressure gradient should be zero	Yes
15. If the flow is layered, e.g. an inversion is present, the relative thicknesses of the layers must be the same.	Not yet

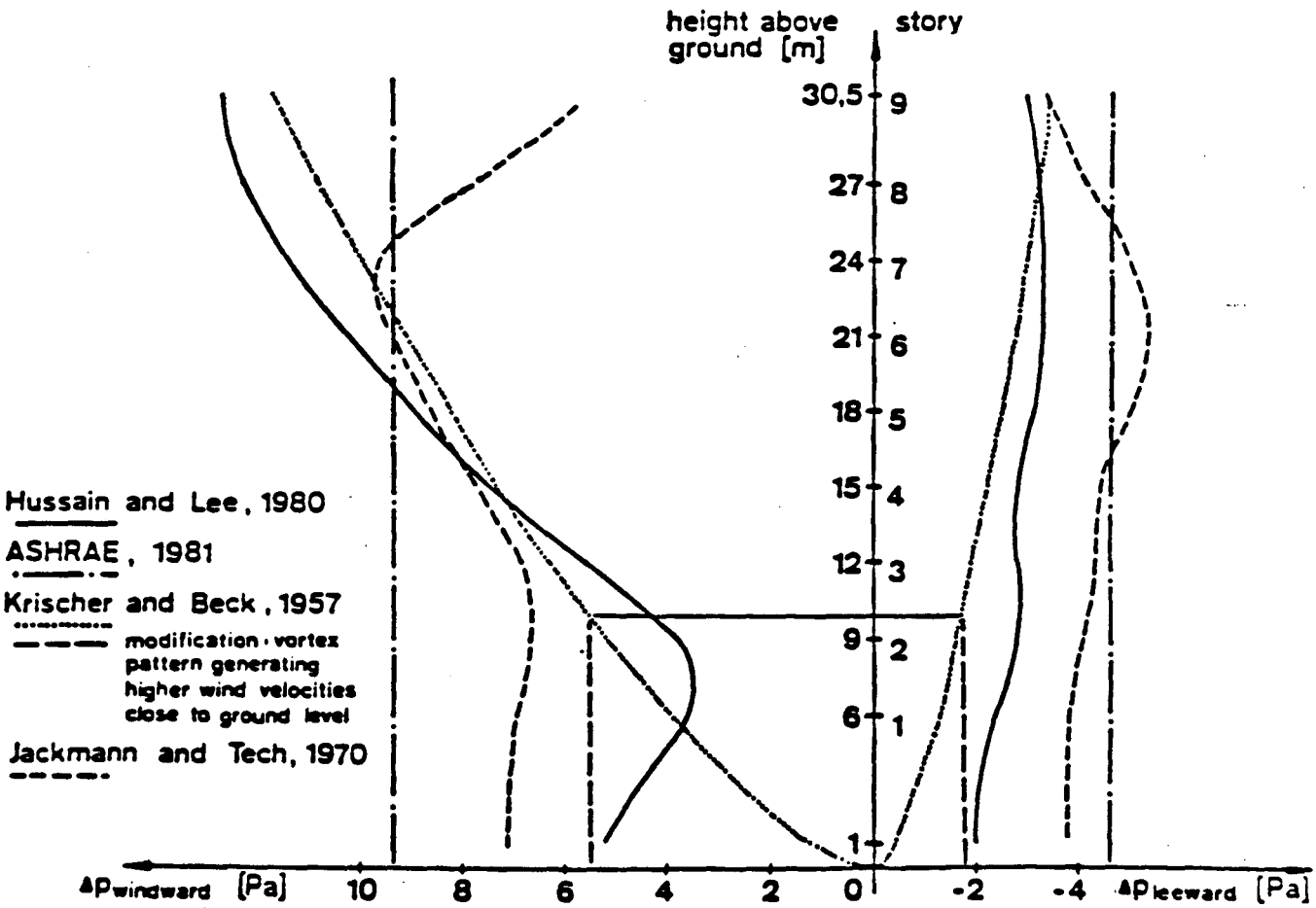

Figure 1: Comparison of the calculated pressure differences for different vertical pressure profiles at wind speed v_{10}= 3 m/s and temperature difference outside/inside of 7 K [4].

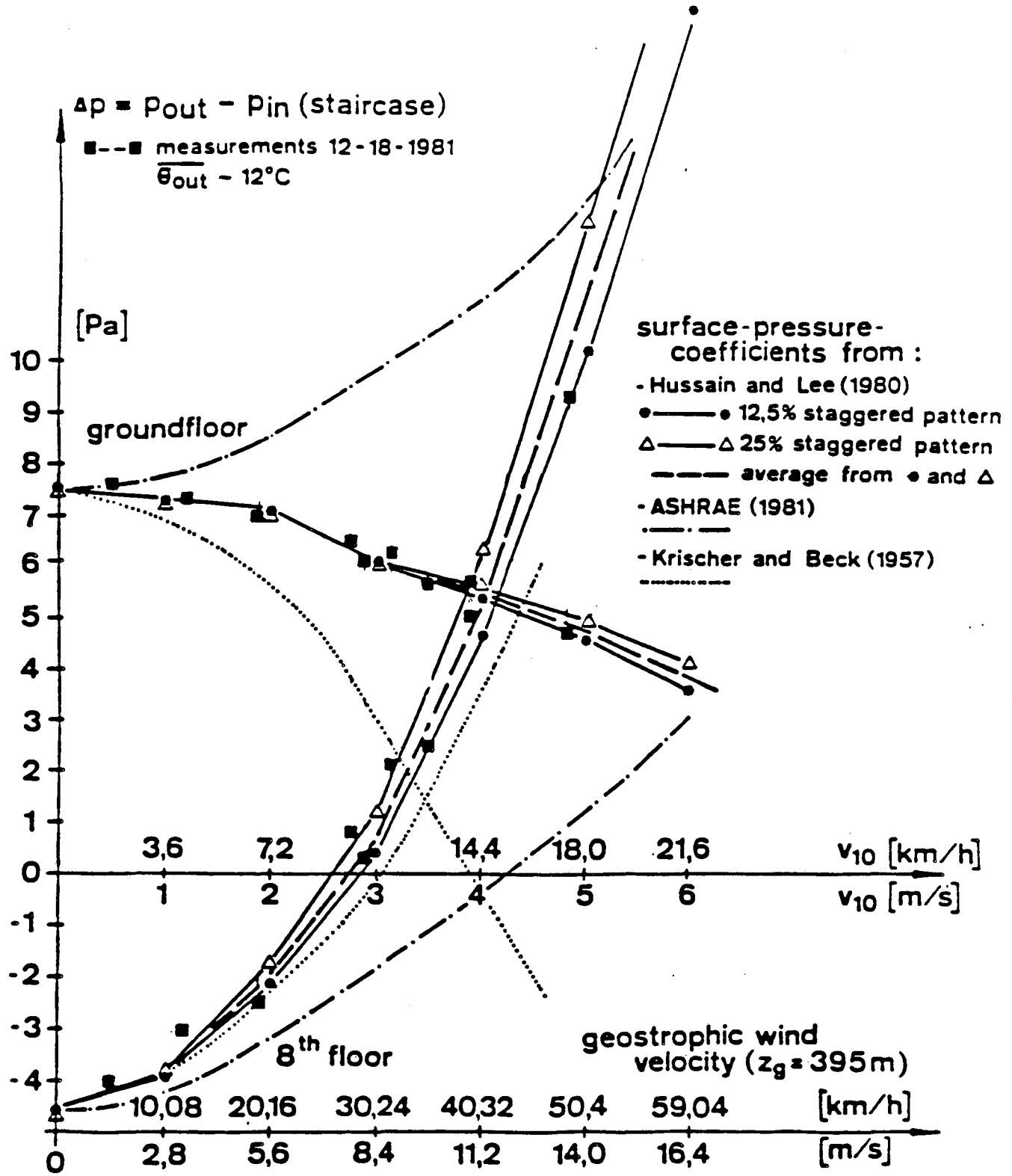

Figure 2: Comparison of the calculated pressure differences at the ground floor and 8th floor for different surface pressure profiles. The temperature difference between inside and outside was 7 K, at a wind speed v_{10}=3 m/s.

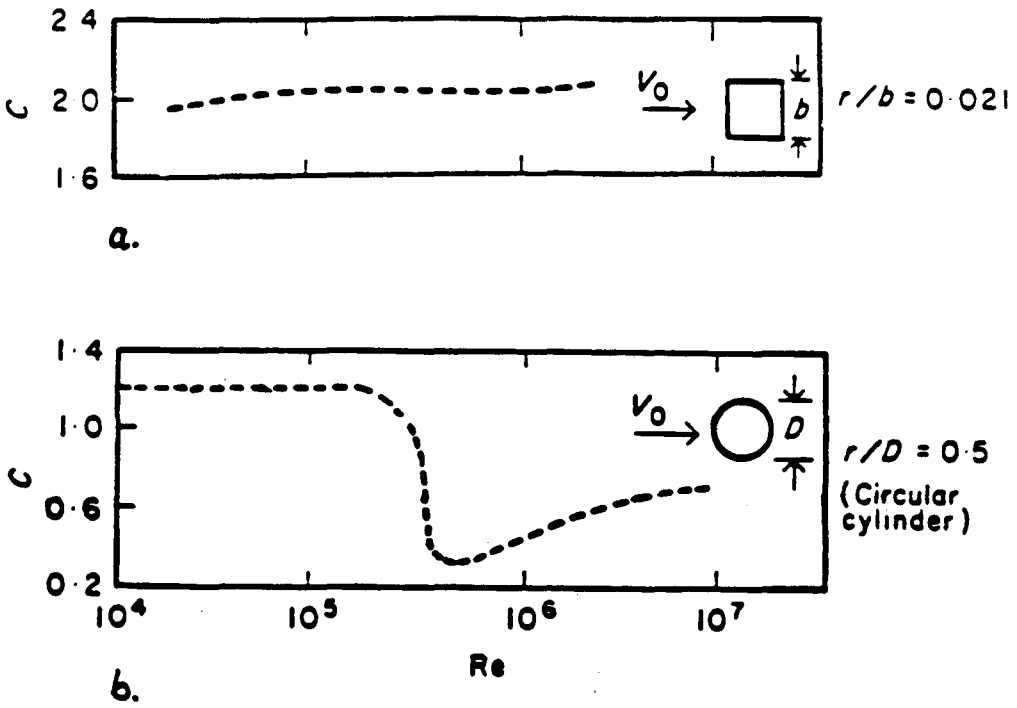

Figure 3: Influence of the Reynolds number on pressure coefficients at two different shapes of buildings [5].

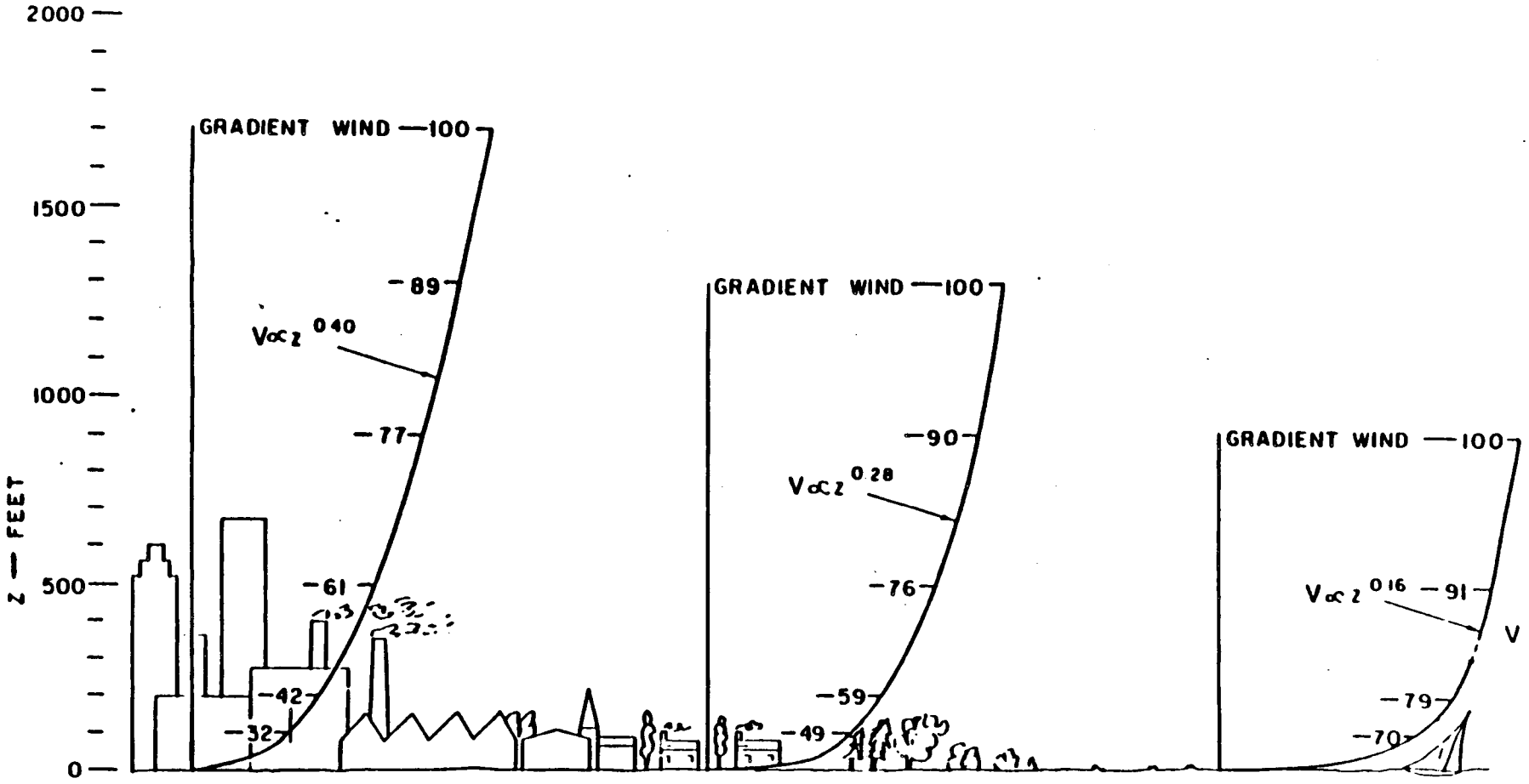

Figure 4: Profiles of mean wind velocity over level terrains of differing roughness [27].

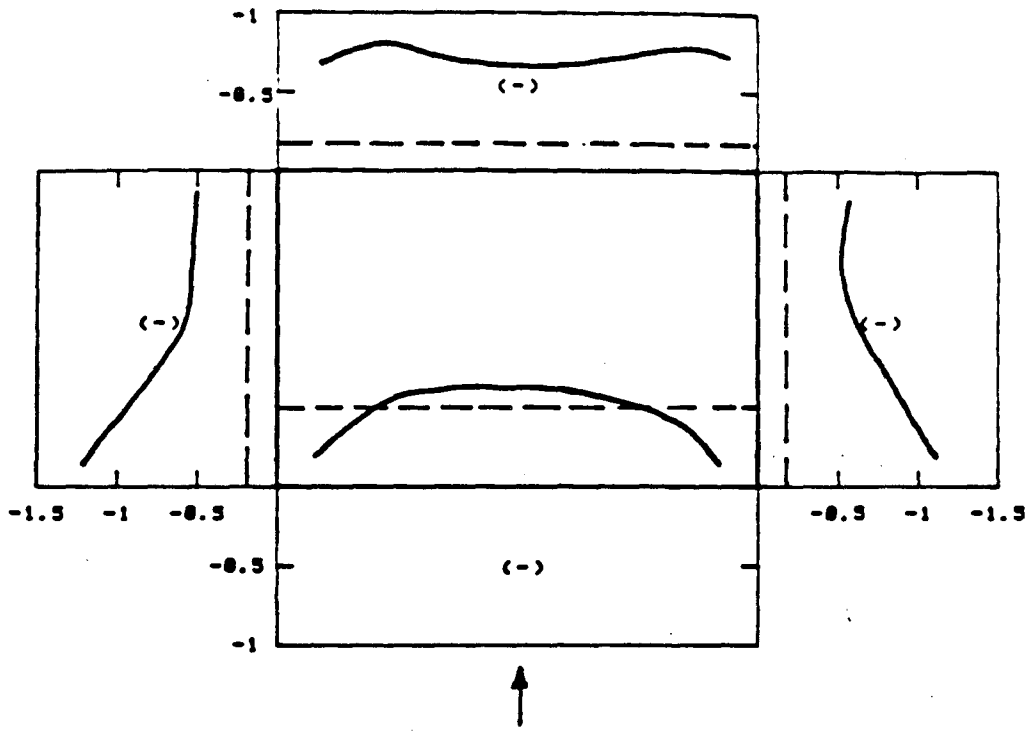

Figure 5: Comparison of pressure coefficients from Wiren [14] Krischer and Beck [13] Wind direction 0 °

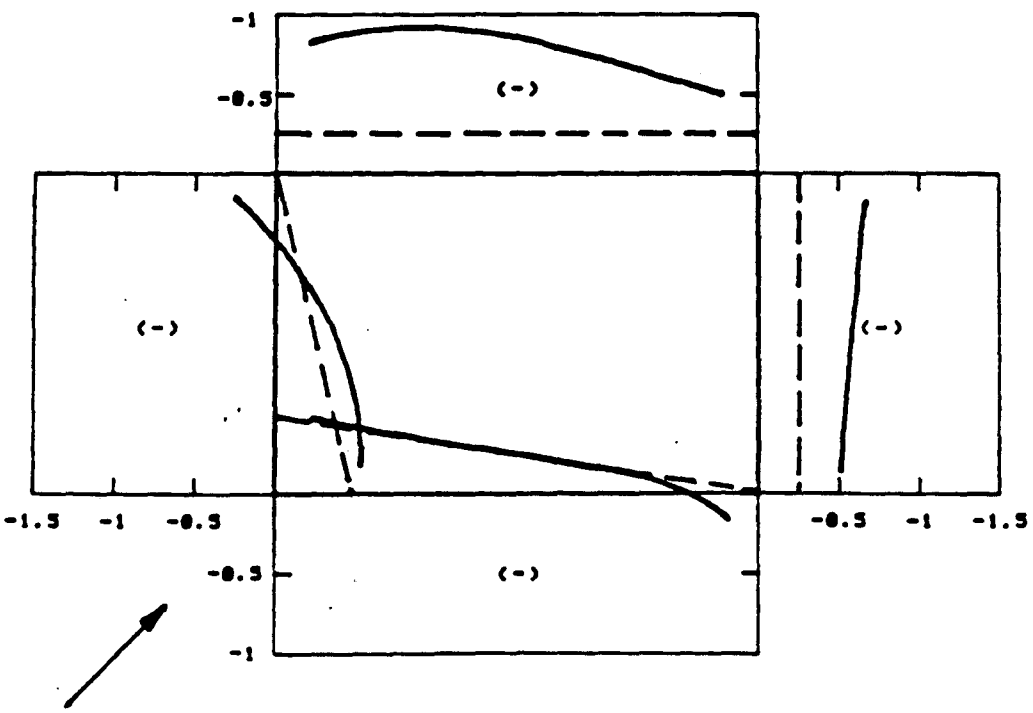

Figure 6: Comparison of pressure coefficients from Wiren [14] Krischer and Beck [13] Wind direction 45 °

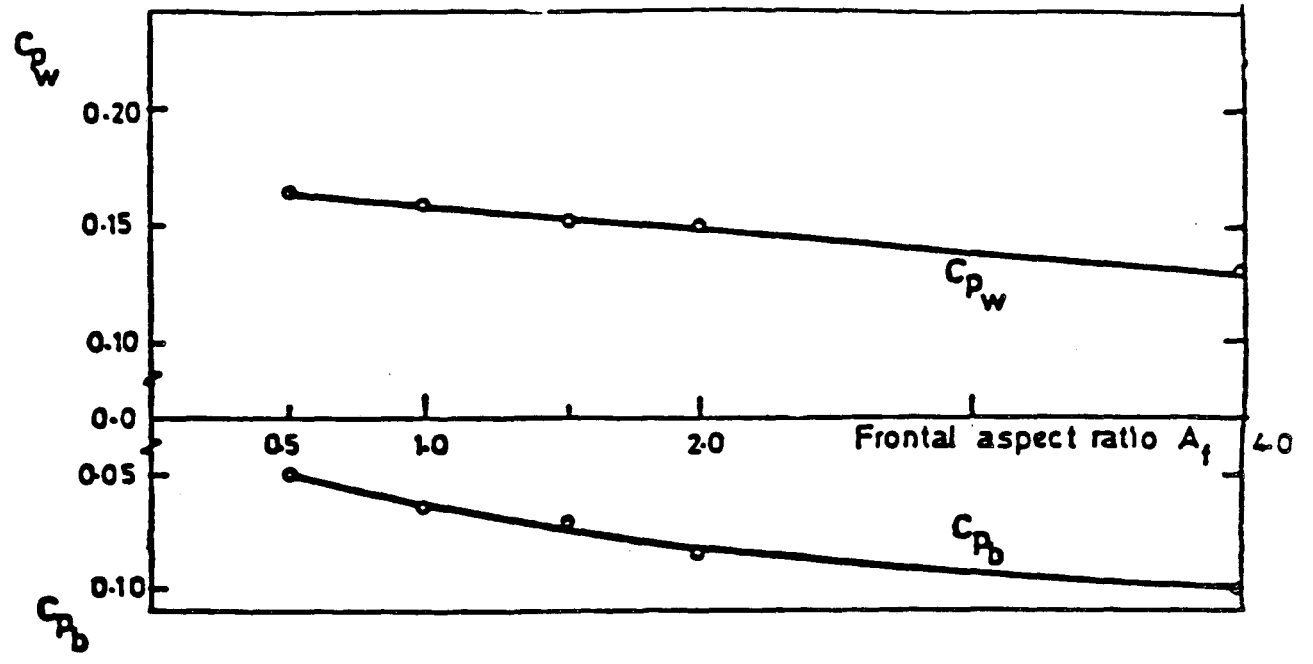

Figure 7: Variation of the Wall Pressure with Frontal Aspect Ratio Isolated Models [22]

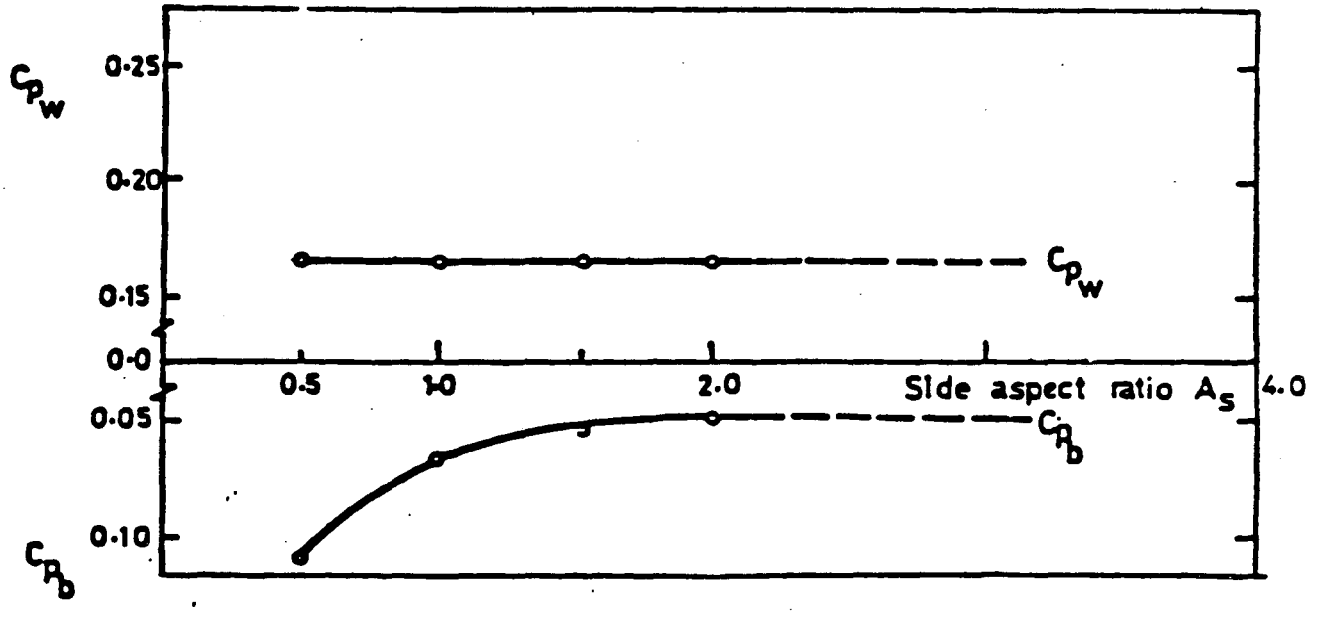

Figure 8: Variation of the Wall Pressure with Side Aspect Ratio Isolated Models [22]

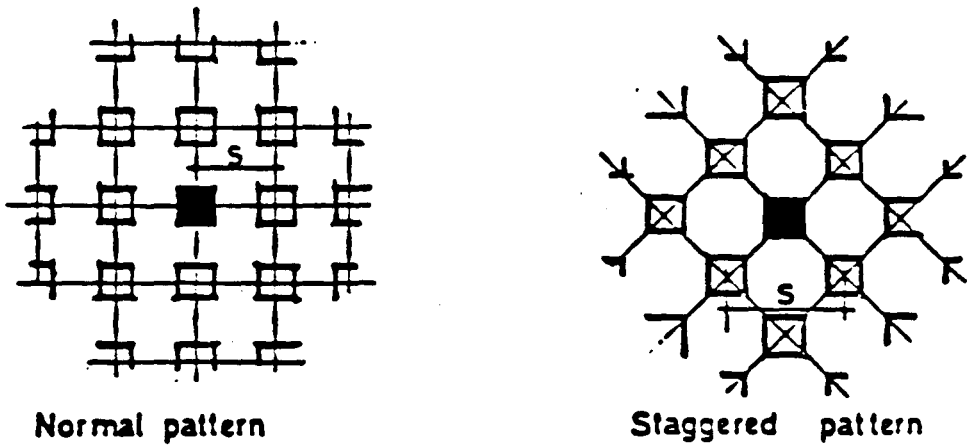

Figure 9: Layout pattern of wind tunnel investigation made by Hussain and Lee [22,23,24].

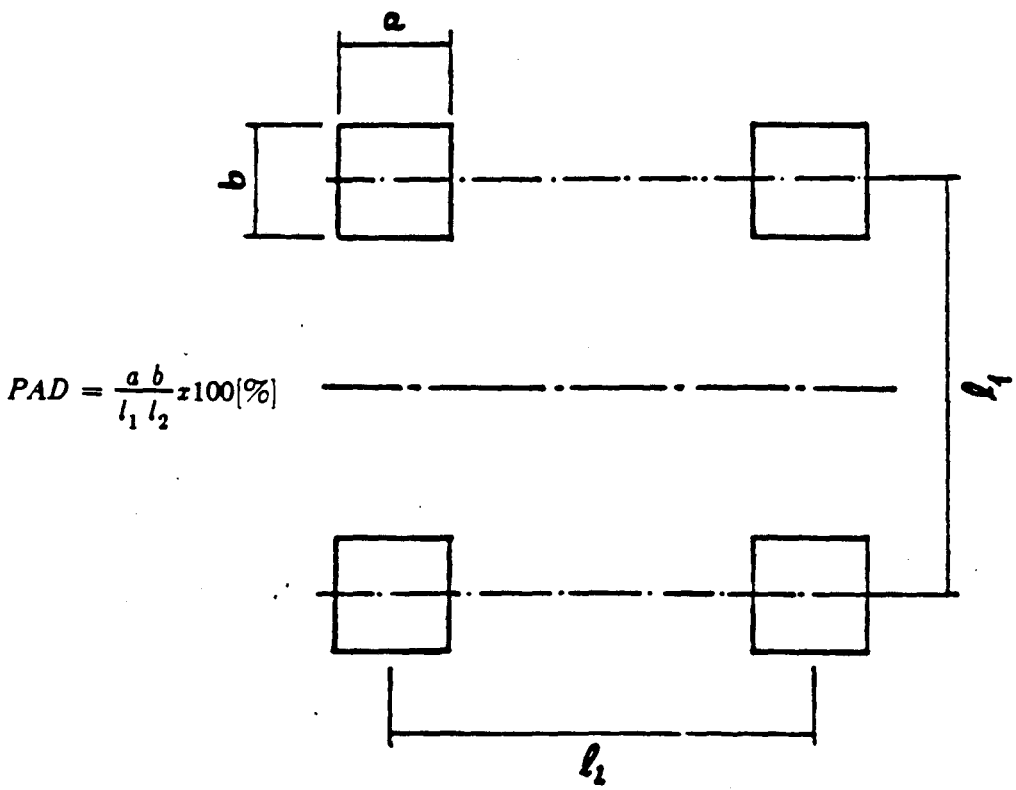

Figure 10: Calculation of the plan area density (PAD) [22]

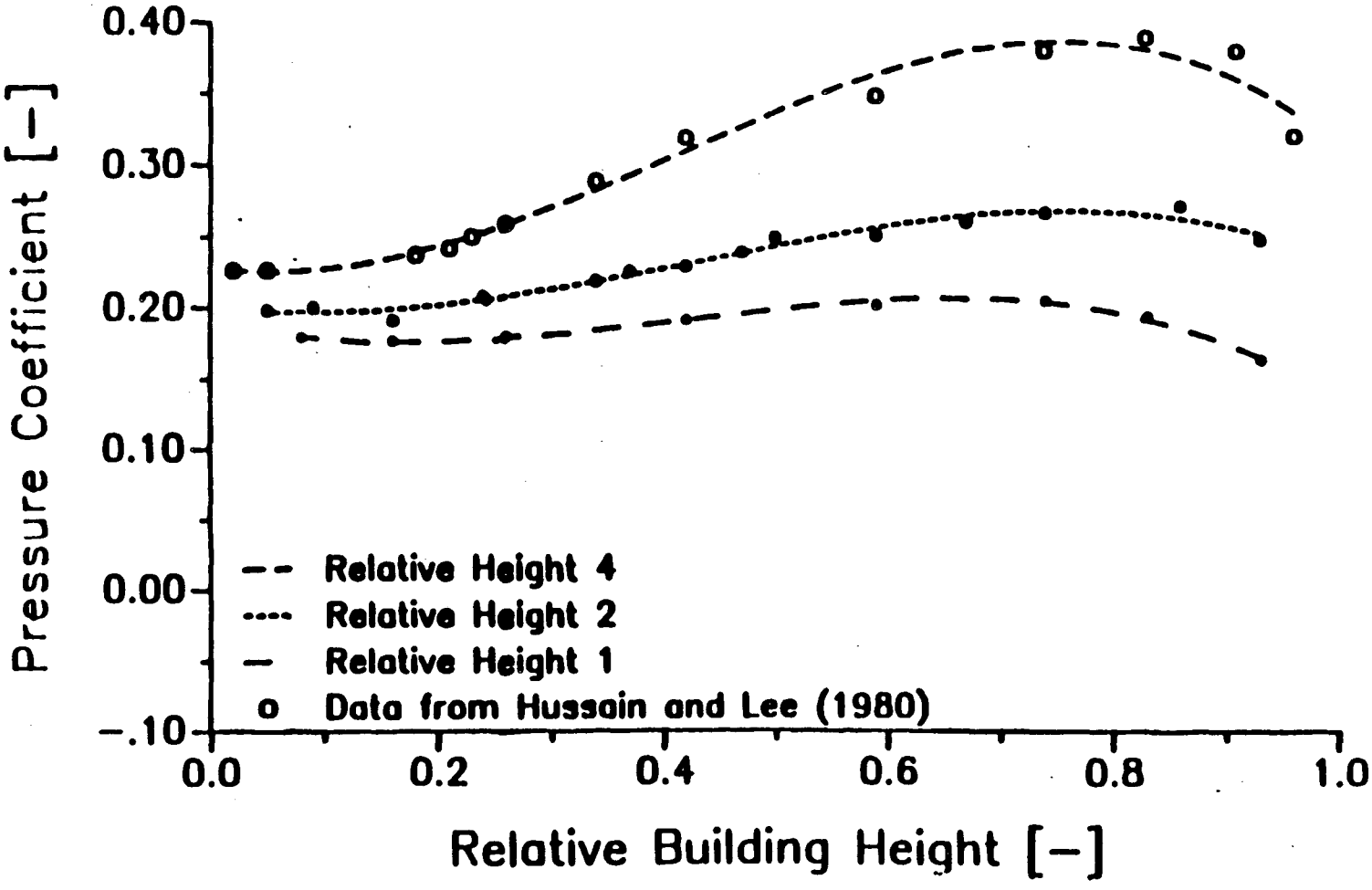

Figure 11: Pressure Coefficient vs. Relative Building Height, 3rd Order Polinomial Fit, PAD=0%, Isolated cube [22]

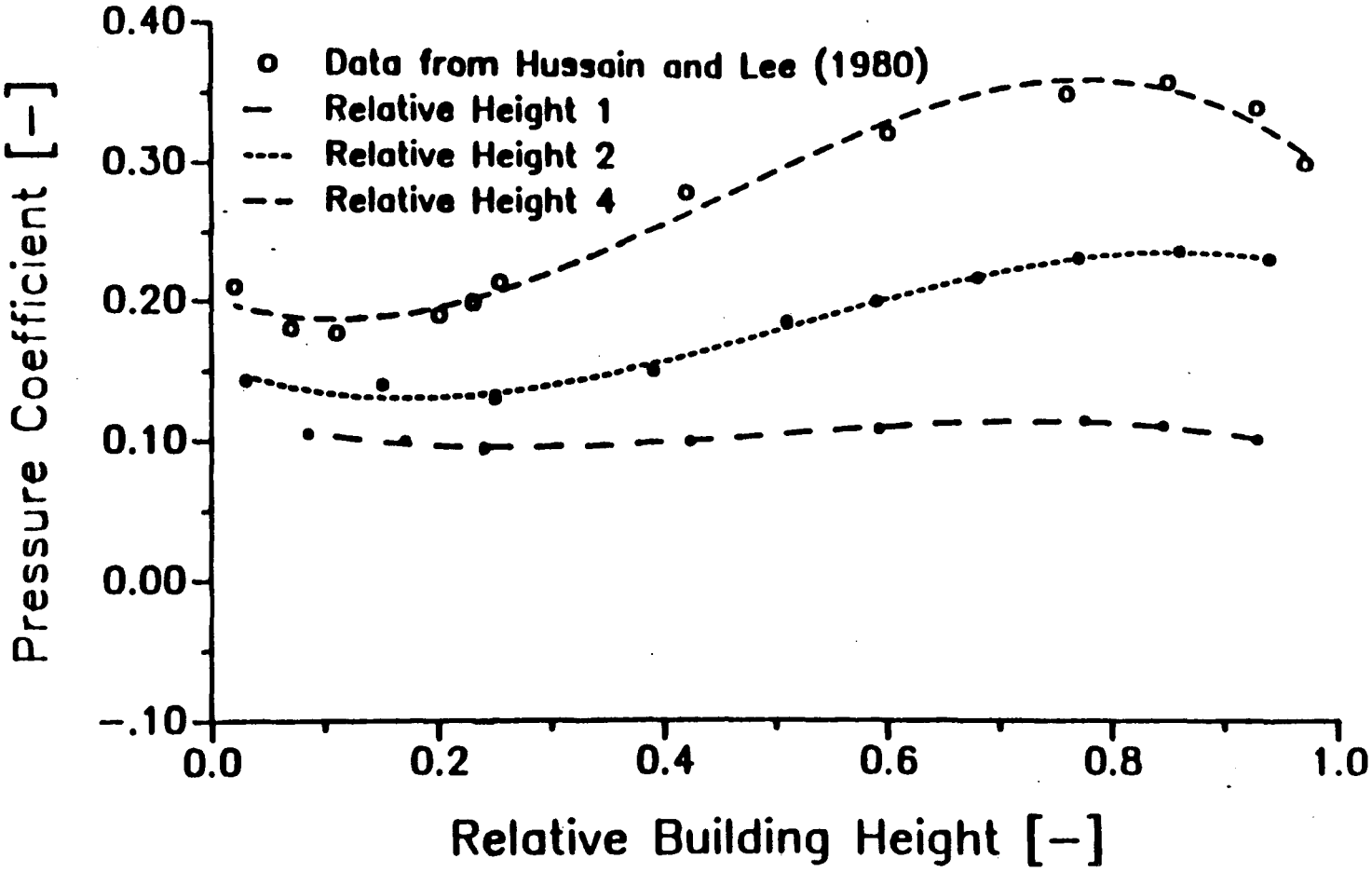

Figure 12: Pressure Coefficient vs. Relative Building Height, 3rd Order Polinomial Fit, PAD=5%, Normal Pattern [23,24]

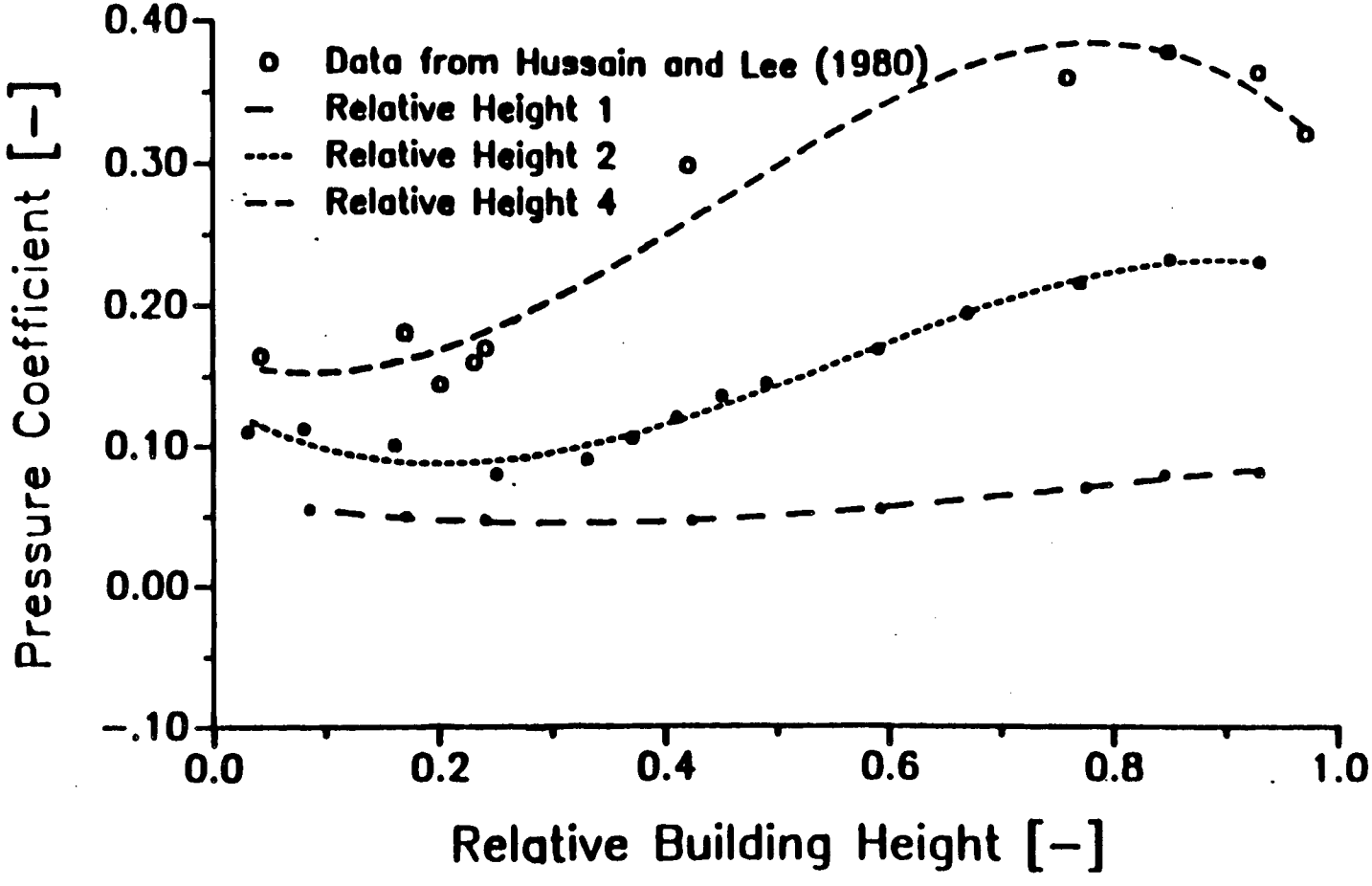

Figure 13: Pressure Coefficient vs. Relative Building Height, 3rd Order Polinomial Fit, PAD=12.5%, Normal Pattern [23,24]

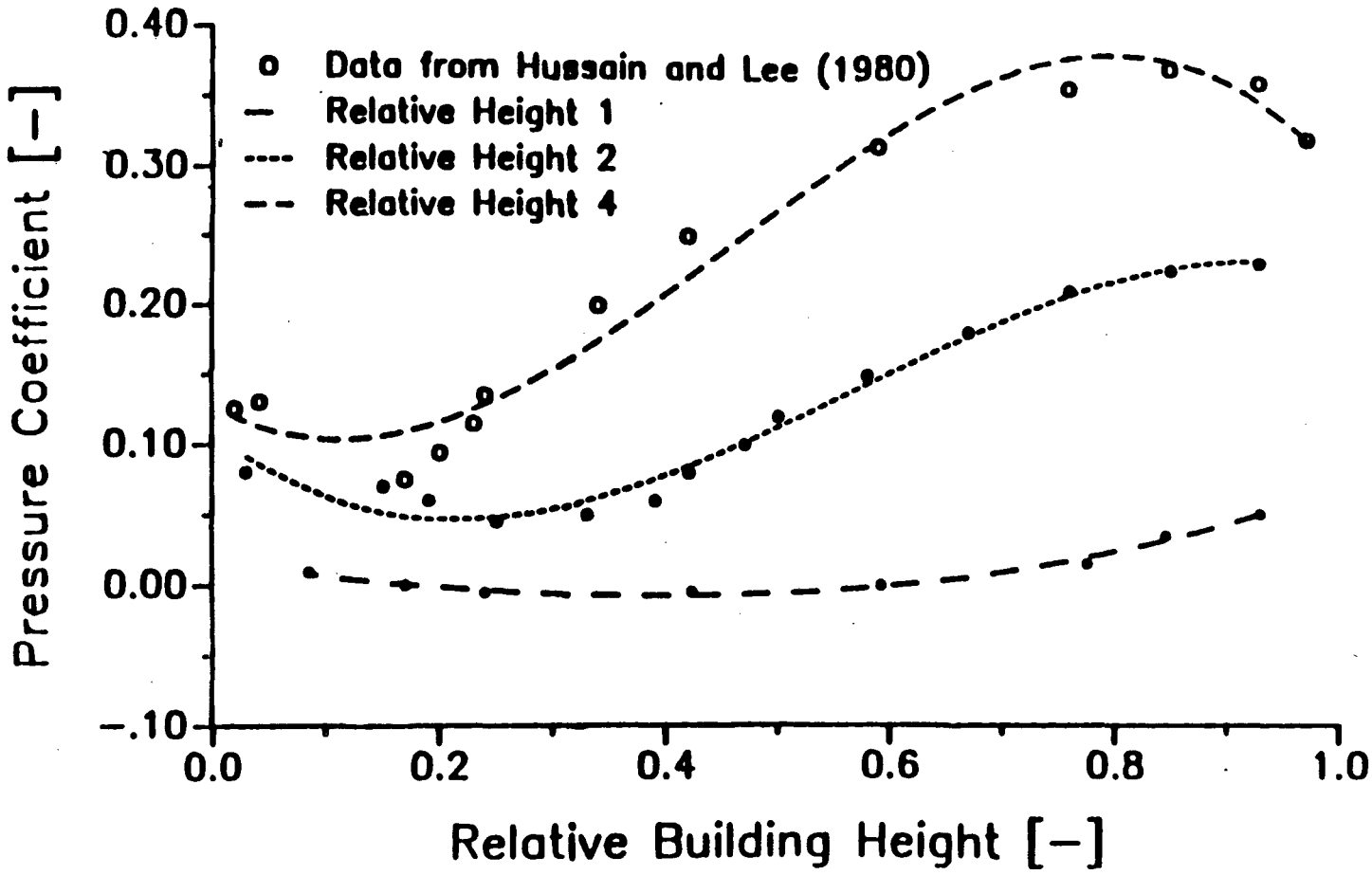

Figure 14: Pressure Coefficient vs. Relative Building Height, 3rd Order Polinomial Fit, PAD=25%, Normal Pattern [23,24]

Table 3: Coefficients for 3rd Order Polinomial Fit
Windward Side, Isolated Cube, PAD = 0%

Relative Height h	Coefficients			
	a_0	a_1	a_2	a_3
0.5	.154540	-.286150	.915204	-.687586
0.8	.201214	-.416627	1.162534	-.848613
0.9	.187089	-.191991	.725393	-.609433
1.0	.194279	-.224608	.800893	-.648879
1.1	.192199	-.163927	.672268	-.564629
1.2	.184967	-.157432	.678678	-.567526
1.3	.189148	-.172628	.712402	-.583227
1.4	.189993	-.134621	.647252	-.544791
1.5	.198633	-.176607	.721683	-.562393
1.7	.194644	-.121555	.649224	-.534967
2.0	.202040	-.124292	.702692	-.561381
3.0	.214894	-.092866	.760366	-.586168
4.0	.228756	-.121375	1.149556	-.939406

Table 4: Coefficients for 3rd Order Polinomial Fit
Windward Side, Normal Pattern, PAD = 5%PAD

Relative Height h	Coefficients			
	a_0	a_1	a_2	a_3
0.5	.086340	-.208884	.516173	-.357584
0.8	.113827	-.253709	.608802	-.409137
0.9	.115641	-.213621	.553267	-.383792
1.0	.120464	-.214460	.549724	-.368114
1.1	.124515	-.233790	.642200	-.443807
1.2	.120029	-.163832	.504512	-.347007
1.3	.126979	-.193235	.593074	-.402809
1.4	.129869	-.195144	.642851	-.439644
1.5	.140334	-.264133	.857486	-.575575
1.7	.164456	-.431569	1.254848	-.821045
2.0	.154065	-.290093	1.006756	-.650526
3.0	.189885	-.416877	1.746460	-1.271403
4.0	.202182	.295928	1.544746	-1.161295

Table 5: Coefficients for 3rd Order Polinomial Fit
Windward Side, Normal Pattern, PAD = 6.25%

Relative Height h	Coefficients			
	a_0	a_1	a_2	a_3
0.5	.077820	-.112609	.274473	-.181468
0.8	.091387	-.160208	.444584	-.302896
0.9	.106782	-.187764	.495121	-.324315
1.0	.113059	-.249777	.771194	-.555668
1.1	.114489	-.190807	.597193	-.352739
1.2	.105628	-.113871	.401663	-.255195
1.3	.111171	-.098356	.383191	-.233552
1.4	.114227	-.140927	.541250	-.346661
1.5	.131371	-.294403	.858280	-.510761
1.7	.147765	-.336023	1.036820	-.633410
2.0	.162727	-.432815	1.359598	-.873213
3.0	.182980	-.429239	1.737719	-1.237560
4.0	.198526	-.326641	1.709435	-1.305427

Table 6: Coefficients for 3rd Order Polinomial Fit
Windward Side, Normal Pattern, PAD = 12.5%

Relative Height h	Coefficients			
	a_0	a_1	a_2	a_3
0.5	.057343	-.157720	.283849	-.146878
0.8	.065565	-.140575	.271511	-.142413
0.9	.577835	-.087243	.131206	-.036854
1.0	.066133	-.145317	.290754	-.124060
1.1	.071832	-.126391	.220455	-.054908
1.2	.068478	-.067123	.135589	-.000825
1.3	.075708	-.112961	.259656	-.067573
1.4	.083344	-.165230	.431583	-.171853
1.5	.105655	-.354145	.918834	-.494385
1.7	.127503	-.492716	1.285401	-.727033
2.0	.131562	-.468477	1.413840	-.855618
3.0	.160837	-.506707	1.969937	-1.357346
4.0	.164198	-.280654	1.791251	-1.371922

Table 7: Coefficients for 3rd Order Polinomial Fit
Windward Side, Normal Pattern, PAD = 25%

Relative Height h	Coefficients			
	a_0	a_1	a_2	a_3
0.5	-.003597	-.073307	.102023	-.040317
0.8	.000451	-.065859	.596631	.006521
0.9	.002775	-.041527	-.027229	.086139
1.0	.015509	-.099568	.074734	.078106
1.1	.016468	-.029998	-.159476	.281859
1.2	.026284	-.081400	.006631	.188936
1.3	.039465	-.180412	.299799	.003804
1.4	.049065	-.253763	.541811	-.168573
1.5	.072125	-.464317	1.103713	-.537035
1.7	.124669	-.814510	1.985846	-1.118533
2.0	.108482	-.622589	1.786887	-1.048199
3.0	.117096	-.521435	2.110980	-.142399
4.0	.127813	-.455261	2.321951	-1.698084

Table 8: Coefficients for 3rd Order Polinomial Fit
Leeward Side, Isolated Cube, PAD = 0%

Relative Height h	Coefficients			
	a_0	a_1	a_2	a_3
0.5	-.030435	-.193621	.408162	-.243179
0.8	-.034141	-.220380	.397314	-.204296
0.9	-.047331	-.160721	.284356	-.140962
1.0	-.060626	-.073240	.066493	.002821
1.1	-.080984	.061472	-.258586	.216912
1.2	-.079516	.045682	-.209580	.175026
1.3	-.083076	.042194	-.208327	.171695
1.4	-.081705	.008725	-.156617	.149977
1.5	-.087093	.023917	-.201287	.181019
1.7	-.099479	.055249	-.267239	.219230
2.0	-.106987	.066355	-.294924	.226016
3.0	-.151026	.099512	-.298876	.182897
4.0	-.171911	.024916	-.144979	.080028

Table 9: Coefficients for 3rd Order Polinomial Fit
Leeward Side, Normal Pattern, PAD = 5%

Relative Height h	Coefficients a_0	a_1	a_2	a_3
0.5	-.043422	-.006240	-.109382	.125845
0.8	-.037940	-.078738	.059988	0
1.1	-.051850	.001613	-.132345	.112912
1.2	-.068936	.099157	-.320611	.218191
1.3	-.076814	.114342	-.337413	.224539
1.4	-.080021	.128107	-.393603	.267204
1.5	-.073802	.134512	-.385219	.254831
1.7	-.072736	-.020422	-.058996	.048888
3.0	-.132352	-.006056	.036125	-.019469
4.0	-.154668	-.078381	.036125	-.019469

Table 10: Coefficients for 3rd Order Polinomial Fit
Leeward Side, Normal Pattern, PAD = 6.25%

Relative Height h	Coefficients a_0	a_1	a_2	a_3
0.5	-.024666	-.014688	-.075865	.112495
0.8	-.032909	-.045646	.047432	0
0.9	-.041123	.026408	-.139504	.123412
1.0	-.043205	.022673	-.133994	.125701
1.1	-.045709	.032747	-.150189	.129689
1.2	-.053562	.080461	-.272668	.217280
1.3	-.064358	.116425	-.319348	.229675
1.4	-.072941	.177388	-.422191	.278006
1.5	-.076297	.138974	-.329023	.219301
1.7	-.073522	.120323	-.312241	.211473
2.0	-.080849	.039151	-.187079	.129928
3.0	-.127452	.034225	-.126366	.062522
4.0	-.148370	-.122413	.124527	-.058441

Table 11: Coefficients for 3rd Order Polinomial Fit
Leeward Side, Normal Pattern, PAD = 12.5%

Relative Height h	Coefficients			
	a_0	a_1	a_2	a_3
0.5	-.013671	.071458	-.262856	.219321
0.8	-.008234	-.031897	-.048373	.219321
0.9	-.014456	-.010428	-.054578	.066011
1.0	-.015709	-.036693	.014085	.023565
1.1	-.011526	-.087186	.115706	-.041669
1.2	-.033935	.091158	-.258616	.182123
1.3	-.038668	.105664	-.286096	.197796
1.4	-.057029	.157540	-.372813	.243049
1.5	-.049024	.105293	-.259276	.174122
1.7	-.035396	-.062035	.093725	-.038572
2.0	-.057959	.035863	-.127790	.099608
3.0	-.091682	-.078541	.166024	-.101812
4.0	-.113437	-.169304	.262029	-.125984

Table 12: Coefficients for 3rd Order Polinomial Fit
Leeward Side, Normal Pattern, PAD = 25%

Relative Height h	Coefficients			
	a_0	a_1	a_2	a_3
0.5	-.018922	.207399	-.627941	.471985
0.8	.013328	-.166835	.180715	-.047463
0.9	-.008210	-.022622	-.153230	.170356
1.0	-.016025	-.045838	-.013598	.054079
1.1	-.038945	.097428	-.315564	.235409
1.2	-.028679	.019299	-.165401	.147484
1.3	-.037181	.081619	-.291688	.215974
1.4	-.041966	.066509	-.218692	.167932
1.5	-.046687	.090328	-.268391	.196236
1.7	-.040225	-.033746	.005069	.002679
2.0	-.054386	.042935	-.214002	.178370
3.0	-.063607	-.183243	.234351	-.086388
4.0	-.072792	-.398448	.553449	-.233620

Table 13: Coefficients for 3rd Order Polinomial Fit
Windward Side, Staggered Pattern, PAD = 10%

Relative Height h	Coefficients a_0	a_1	a_2	a_3
0.5	.075147	-.193114	.426528	-.277051
0.8	.073854	-.142314	.339219	-.221497
0.9	.081962	-.156714	.391081	-.267261
1.1	.091709	-.174605	.447347	-.292797
1.2	.090217	-.123348	.361225	-.238819
1.3	.105879	-.182882	.455130	-.276256
1.4	.094810	-.128195	.404714	-.252425
1.5	.108020	-.203234	.577497	-.348418
1.7	.135360	-.375117	1.016469	-.622457
2.0	.123428	-.300597	.957993	-.595899
3.0	.146487	-.373647	1.536569	-1.052089
4.0	.168670	-.402431	1.908485	-1.397824

Table 14: Coefficients for 3rd Order Polinomial Fit
Windward Side, Staggered Pattern, PAD = 12.5%

Relative Height h	Coefficients a_0	a_1	a_2	a_3
0.5	.052570	-.159014	.365068	-.238166
0.8	.074681	-.154352	.339591	-.213607
0.9	.060514	-.031050	.067005	-.036169
1.1	.085302	-.199720	.466950	-.283757
1.2	.083182	-.121066	.285512	-.156894
1.3	.072337	-.044123	.183130	-.100380
1.4	.082993	-.125578	.350851	-.181651
1.5	.091016	-.214557	.587866	-.327543
1.7	.122670	-.395984	1.040056	-.615384
2.0	.118736	-.333600	1.016529	-.607422
3.0	.141577	-.455434	1.708129	-1.133775
4.0	.168130	-.514621	2.241836	-1.622729

Table 15: Coefficients for 3rd Order Polinomial Fit
Windward Side, Staggered Pattern, PAD = 25%

Relative Height h	Coefficients			
	a_0	a_1	a_2	a_3
0.5	-.002503	-.046087	.050296	0
0.8	.008597	-.041688	-.019935	.088159
0.9	.017427	-.088514	.065617	.053308
1.0	.038221	-.234721	.434697	-.181128
1.1	.014692	-.032141	-.043521	.142961
1.2	.016471	-.039448	.002057	.125020
1.3	.023729	-.062854	.061311	.109322
1.4	.046682	-.211203	.450573	-.147121
1.5	.054297	-.266125	.590827	-.231368
1.7	.095407	-.564772	1.342088	-.712748
2.0	.101237	-.587105	1.570564	-.889766
3.0	.128632	-.618990	2.119621	.1.365209
4.0	.139887	-.569123	2.447520	-1.717308

Table 16: Coefficients for 3rd Order Polinomial Fit
Windward Side, Staggered Pattern, PAD = 40%

Relative Height h	Coefficients			
	a_0	a_1	a_2	a_3
0.5	-.029538	-.002522	-.043755	.055686
0.8	-.017145	-.042222	-.011133	.065553
0.9	-.012060	-.033687	-.067288	.122856
1.0	-.000412	-.115055	.121956	.043577
1.1	.007537	-.072738	-.053609	.193361
1.2	-.001429	.015913	-.252665	.362306
1.3	.018163	-.096101	.082308	.128808
1.4	.034512	-.210919	.324482	.014777
1.5	.047112	-.283672	.592707	-.184342
1.7	.096638	-.701396	1.592255	-.816326
2.0	.094841	-.691917	1.772998	-.980363
3.0	.121277	-.733851	2.480842	-1.621495
4.0	.122320	-.595649	2.735673	-2.002234

Table 17: Coefficients for 3rd Order Polinomial Fit
Leeward Side, Staggered Pattern, PAD = 0%

Relative Height h	Coefficients a_0	a_1	a_2	a_3
0.5	.009418	-.045715	.0342132	0
0.8	.006695	-.059871	.0425502	0
0.9	-.004081	.016628	-.155489	.136024
1.1	-.009737	.046694	-.233086	.184777
1.2	-.015976	.056080	-.205912	.149383
1.3	-.021750	.051618	-.198882	.144556
1.4	-.031696	.128828	-.354513	.233388
1.5	-.030740	.094419	-.273819	.179316
1.7	-.025256	-.000765	-.067955	.053444
2.0	-.042926	.060292	-.212956	.140837
3.0	.079724	-.019673	-.034606	.027807
4.0	-.091742	-.210289	.245770	-.100894

Table 18: Coefficients for 3rd Order Polinomial Fit
Leeward Side, Staggered Pattern, PAD = 12.5%

Relative Height h	Coefficients a_0	a_1	a_2	a_3
0.5	-.004095	.084052	-.292264	.237124
0.8	.003876	-.032413	-.038848	.070075
0.9	.013187	-.077672	.049044	.010807
1.1	.003372	-.047005	.000017	.027130
1.2	-.013692	.069283	-.231795	.161016
1.3	-.022531	.128825	-.362761	.242667
1.4	-.031940	.139790	-.356791	.231714
1.5	-.028822	.110039	-.311258	.210119
1.7	-.017226	-.025909	-.024065	.031214
2.0	-.034105	.023012	-.125647	.090894
3.0	-.066653	-.053831	.018056	.011887
4.0	-.074533	-.206196	.165695	-.018175

Table 19: Coefficients for 3rd Order Polinomial Fit
Leeward Side, Staggered Pattern, PAD = 25%

Relative Height h	Coefficients			
	a_0	a_1	a_2	a_3
0.5	.020225	-.078854	.038947	.032352
0.8	.015837	-.097600	.085100	0
0.9	.007213	-.075182	.053324	.009963
1.0	.007861	-.108994	.139530	-.045543
1.1	-.007608	-.015869	-.063611	.082250
1.2	-.012344	-.005711	-.120817	.134953
1.3	-.018988	.008059	-.067934	.072250
1.4	-.015336	-.044372	.046010	0
1.5	-.026310	.022681	-.103903	.095477
1.7	-.020810	-.047758	.041874	.007248
2.0	-.026863	-.039929	.012738	.027078
3.0	-.046186	-.138078	.129487	-.010648
4.0	-.059981	-.409769	.712128	-.370480

Table 20: Coefficients for 3rd Order Polinomial Fit
Leeward Side, Staggered Pattern, PAD = 40%

Relative Height h	Coefficients			
	a_0	a_1	a_2	a_3
0.5	-.003084	-.013080	-.033232	.055689
0.8	-.008255	.005691	-.105852	.101726
0.9	-.016715	.026784	-.174457	.155516
1.0	-.007648	-.111952	.176980	-.074308
1.1	-.019002	.004679	-.133547	.125585
1.2	-.031336	.052650	-.204316	.157821
1.3	-.041652	.098819	-.277682	.193428
1.4	-.049891	.124219	-.328234	.223446
1.5	-.049619	.092727	-.248525	.171058
1.7	-.047409	-.020471	-.012377	.032186
2.0	-.058009	.017599	-.118781	.103456
3.0	-.083624	.022789	-.225657	.206498
4.0	-.104259	-.039262	-.207109	.212278

LAWRENCE BERKELEY LABORATORY
TECHNICAL INFORMATION DEPARTMENT
1 CYCLOTRON ROAD
BERKELEY, CALIFORNIA 94720